Supplementary Material

European sulphate aerosols were a key driver of the early twentieth-century intensification of the Asian summer monsoon

Weihao Sun[1,2], Massimo A. Bollasina[1], Ioana Colfescu[3,4], Guoxiong Wu[2] and Yimin Liu[2]

[1]School of GeoSciences, University of Edinburgh, Edinburgh, UK
[2]Key Laboratory of Earth System Numerical Modelling and Application, Institute of Atmospheric Physics, Chinese Academy of Sciences, Beijing, China.
[3]School of Mathematics and Statistics, University of St Andrews, St Andrews, UK
[4]National Centre for Atmospheric Science, UK

Correspondence to: Massimo A. Bollasina (Massimo.Bollasina@ed.ac.uk)

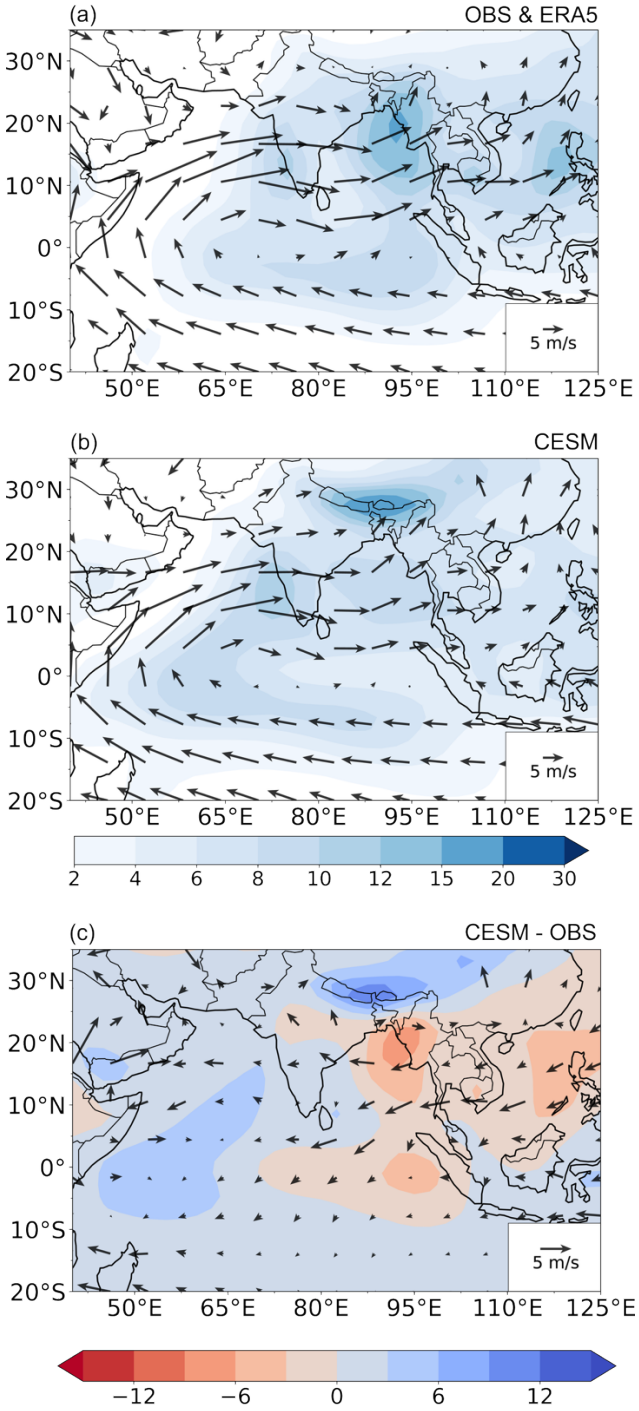

Figure S1. June–August (JJA) climatological (1981-2005) precipitation (mm day^{-1}) and 850-hPa winds (m s^{-1}) from (a) observational datasets (CMAP and ERA5, respectively), (b) the ALL ensemble, and (c) their difference.

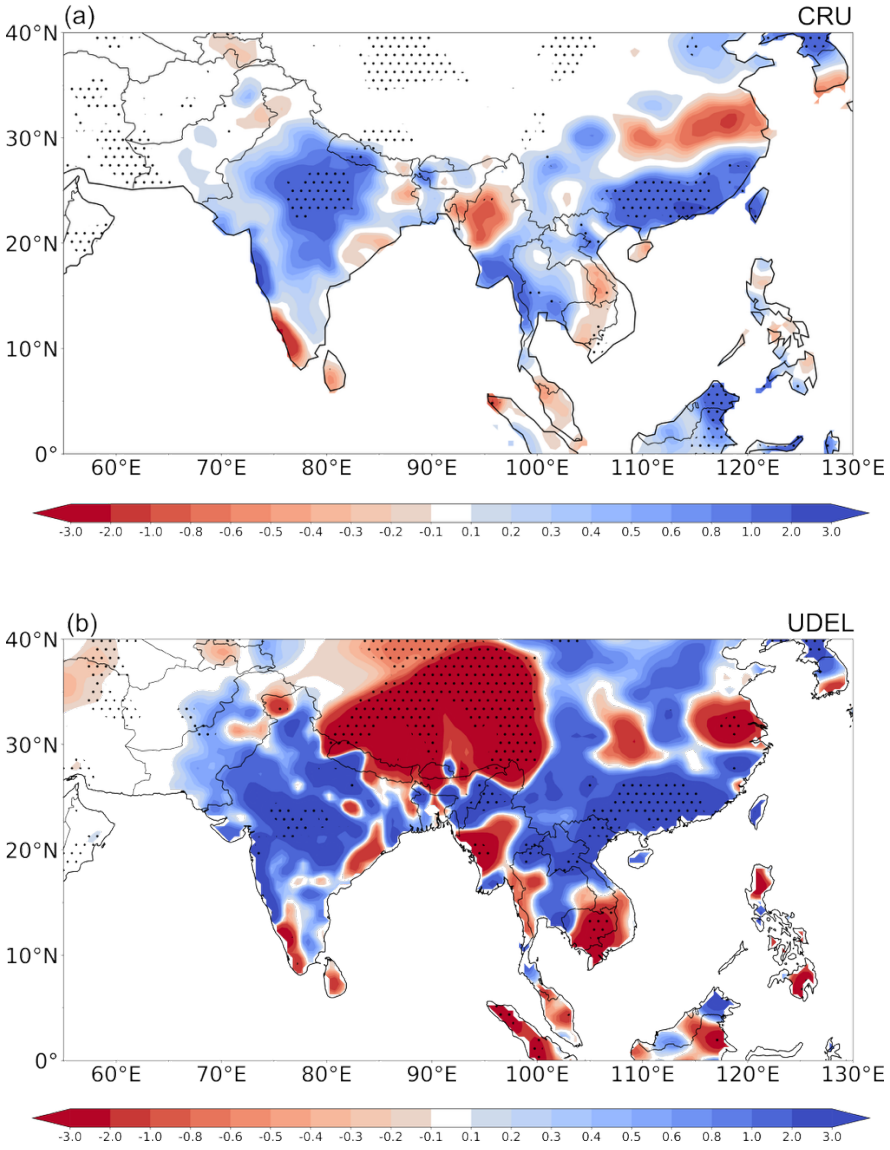

Figure S2. Spatial patterns of the 1901-1955 linear trends of JJA precipitation (mm day^{-1} (55 years)$^{-1}$) for (a) CRU and (b) UDEL observations. The black dots mark the grid points for which the trend exceeds the 90% significance level according to the two-tailed Student's t-test.

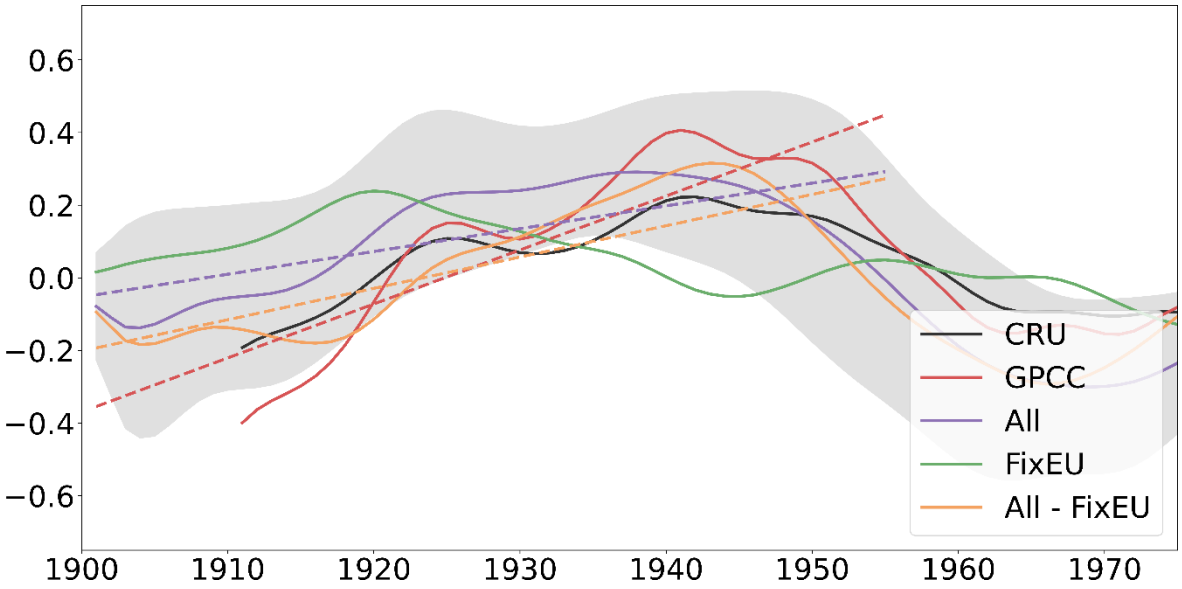

Figure S3. Time series of area-averaged JJA precipitation anomalies (mm day^{-1}; deviations from the 1901-2000 climatology) over southern China (land-only points within 25°–35°E, 110°–120°N) smoothed with 11-year running means to highlight low-frequency (multi-decadal) fluctuations. The black and red lines represent observations (CRU and GPCC, respectively), while the purple, green and orange lines represent the ensemble means of ALL, fixEU, and their difference (EU). The grey shading represents the standard deviation of the eight-member ALL ensemble around the mean. The 1901-1955 least-squares linear trends of the simulated time series are shown as dashed lines in the corresponding colours.

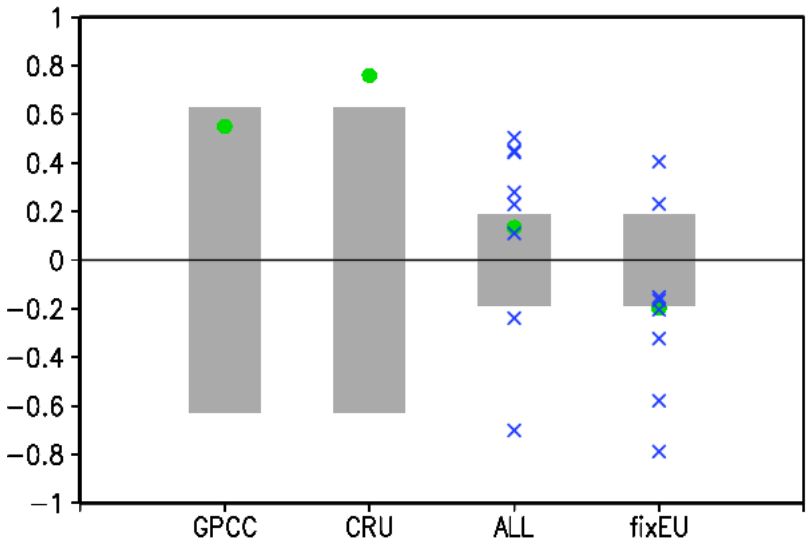

Figure S4. 1901-1955 least-squares linear trends of JJA precipitation (mm day^{-1} (55 years)$^{-1}$) over central-northern India (75°–87°E, 16°–27°N) for observations and the model experiments. The green dots represent the observed or ensemble-mean trends, and blue crosses represent trends of individual ensemble members. The grey bars represent the 90% confidence intervals derived from the PI control run.

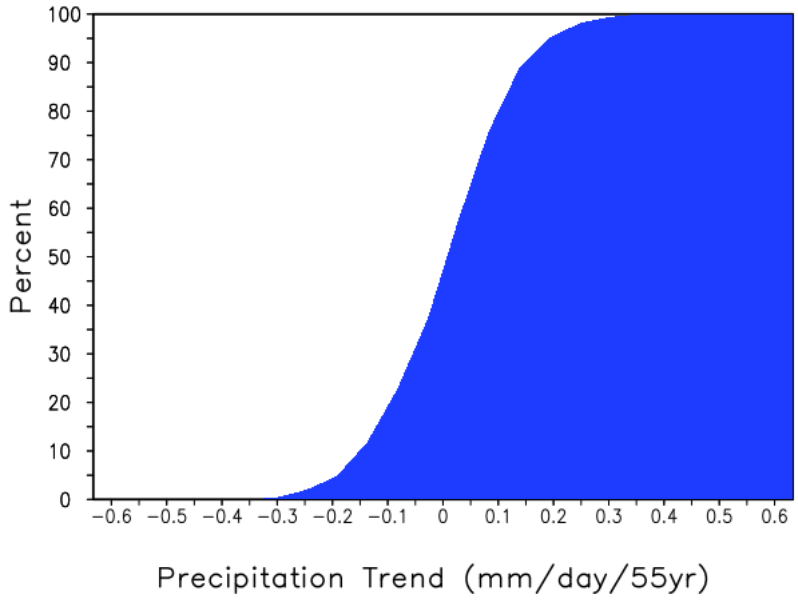

Figure S5. Cumulative probability distribution (%) of the 8-member ensemble-mean 55-year trends of June-August average precipitation (mm day^{-1} (55 years)$^{-1}$) over central-northern India (76°–87°E, 16°–27°N) taken from the PI control run.

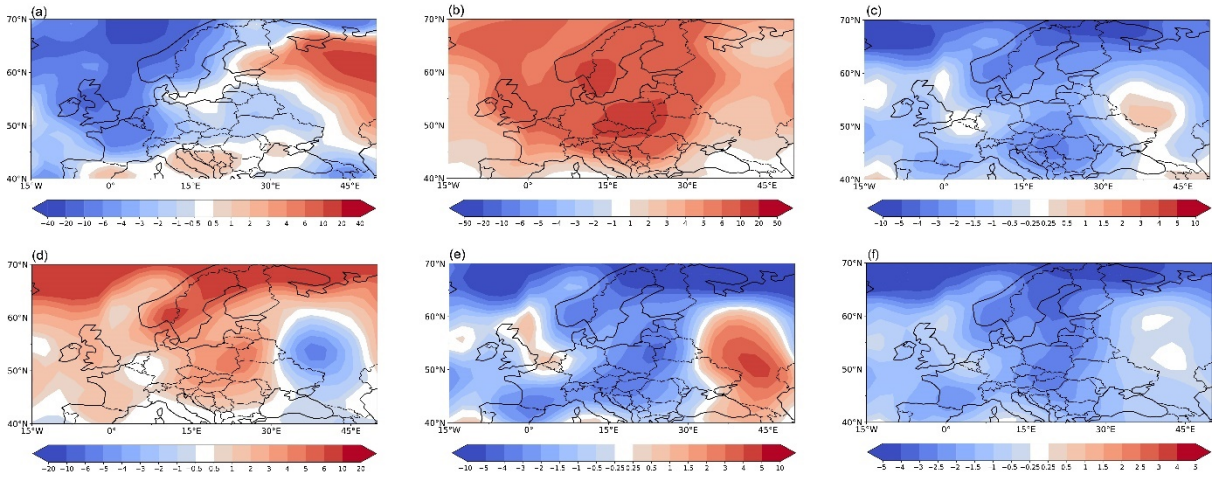

Figure S6. Spatial patterns of the 1901-1955 linear trends of JJA (a) cloud droplet effective radius (10 μm (55 years)$^{-1}$), (b) vertically-integrated cloud droplet concentration (m^{-2} (55 years)$^{-1}$), (c) net radiation at the model top (W m^{-2} (55 years)$^{-1}$), (d) total column liquid water path (10^3 Kg m^{-2} (55 years), (e) surface all-sky downward shortwave radiation (W m^{-2} (55 years)$^{-1}$), and (f) net radiation at the surface (W m^{-2} (55 years)$^{-1}$) associated with increased European sulphate aerosols (difference between the ALL and fixEU ensemble means).

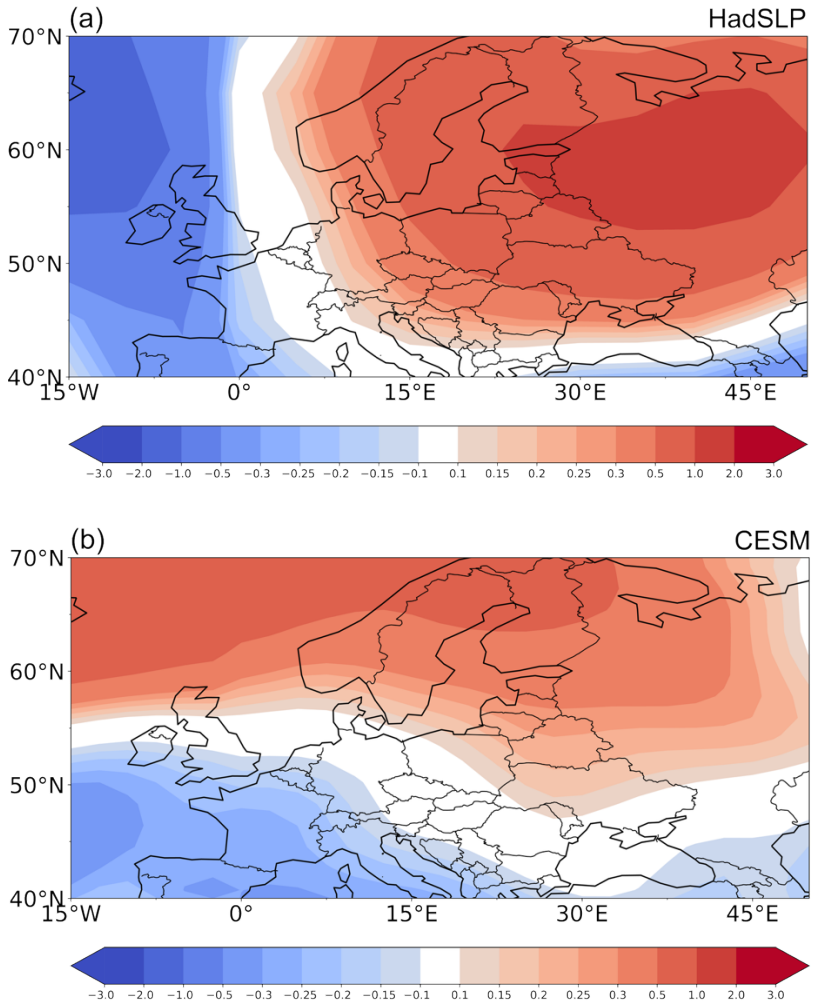

Figure S7. Spatial patterns of the 1901-1955 linear trends of JJA sea-level pressure (hPa (55 years)$^{-1}$) for (a) HadSLP and (b) the all-forcing ensemble (ALL).

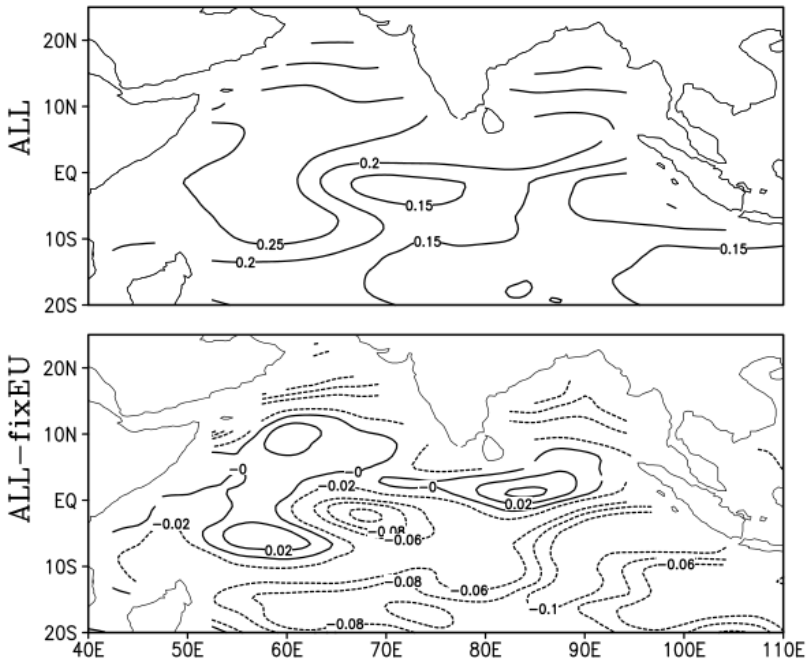

Figure S8. Spatial patterns of the 1901-1955 changes of JJA sea-surface temperature (K) for (a) the all-forcing ensemble (ALL), and (b) the difference between ALL and the all-forcing experiment with fixed preindustrial aerosol emissions over Europe (fixEU), representing the impact of EU aerosols. Changes are calculated as the difference between the (1941-1955) and the (1901-1915) averages.